IMPROVED MODAL IDENTIFICATION FROM BASE EXCITATION VIBRATION TESTS USING MODAL EFFECTIVE PARAMETERS

Nicolas ROY (1), **Fabrice BUFFE** (2)

(1) TOP MODAL, Ecoparc II, av. José Cabanis, 31130 Quint-Fonsegrives, FRANCE
Tel. +33 (0) 5 61 83 59 72 - e-mail nicolas.roy@topmodal.fr

(2) CNES, 18, av. Edouard Belin, 31401Toulouse Cedex 9, FRANCE
Tel. +33 (0) 5 61 28 34 65 - e-mail fabrice.buffe@cnes.fr

ABSTRACT

The RTMVI modal identification method was introduced 10 years ago in order to extract modes from frequency response functions (FRF) obtained from sine-sweep shaker table vibration tests as opposed to classical modal survey tests. Recently, a study funded by the CNES [1] was carried out with the goal of extending the capabilities of the RTMVI method and in particular the ability to identify coupled modes and to assess the quality and reliability of the FRF and the identified modes.

Several state-of-the-art methods in the time and frequency domains were initially evaluated as potential complementary methods to be coupled with the RTMVI approach. However in the end, an extended MDOF version of the RTMVI algorithm proved to be most suitable and best performing solution, and was therefore implemented and validated.

This paper presents the formulation and implementation of the new RTMVI/MDOF method along with an industrial application to illustrate its effectiveness.

1. INTRODUCTION

The majority of modal identification methods [2,3] rely on modal survey tests which are generally performed using one or several small shakers to excite the structure, and accelerometers to measure the responses. The corresponding FRF are therefore accelerances (acceleration/force) from which the dynamic flexibilities (displacement/force) may be derived by dividing by $-\omega^2$.

Unfortunately, modal survey tests are rarely carried out in the context of spacecraft structures since they call for dedicated tests (and facilities) which must be performed in addition to the required vibration qualification tests, whose impact on cost and delays is often incompatible with the project budget and schedule.

To overcome this problem, a study funded by ESA was carried out ten years ago with the objective of reducing spacecraft cost and development time by developing a modal identification method compatible with shaker table tests. The resulting RTMVI method [4,5] allows extracting modes from the corresponding imposed-acceleration FRF including dynamic transmissibilities (acceleration/acceleration) and dynamic masses (force/acceleration) assuming force measurements at the interface are available. Moreover, using a real-mode approach based on modal effective parameters, the RTMVI method combines robustness and efficiency such that modes can be identified quickly - in a matter of minutes - between two successive test runs.

The success of the RMTVI method in the aerospace industry has motivated a new study funded by the CNES and aimed at extending the capabilities of the method, and in particular the ability to identify coupled modes and to assess the quality and reliability of the FRF and the identified modes.

For example, the first bending modes of spacecraft structures are often very close in frequency and may be simultaneously excited during vibration tests in both lateral directions due to coupling effects. Moreover, the difficulty of identifying these coupled modes is often compounded by other undesirable factors related to base excitation vibration tests such as a fast sweep-rate, high excitation levels, local flexibility at the interface and noise in the FRF. Therefore the ability to identify coupled modes goes hand in hand with the ability to assess the quality of the FRF.

At the beginning of the study several state-of-the-art time and frequency domain methods were evaluated as potential complementary methods to be coupled with the RTMVI approach. In parallel, these methods were also used as a basis of comparison for the development of an MDOF version of the RTMVI method which was also developed during the study. In the end, the RTMVI/MDOF algorithm proved to be best solution in terms of performance and ease of use. Moreover, the RTMVI/MDOF algorithm was by far the least sensitive to noise in the FRF.

The RTMVI/MDOF method is based on curve-fitting of the imaginary part of the FRF to directly identify a set of modes within a given frequency range in terms of natural frequency, damping and modal effective parameters. The use of singular value decomposition (SVD) has been implemented to facilitate and improve FRF assessment and subsequent modal identification, particularly useful when dealing with a large number of FRF.

The paper starts with a review of the fundamentals concerning modal effective parameters and mode superposition. Next a brief description of modal identification methods considered in this study is presented and in particular the RFP (Rational Fraction Polynomial) method and the RTMVI/MDOF method developed during the study. Finally an industrial case study involving the PICARD micro-satellite is presented to illustrate the interest and effectiveness of the RTMVI/MDOF method.

2. MATRIX NOTATION

A matrix is designated using a bold face character along with indices relating to its rows and columns (e.g. $\mathbf{X}_{ij}$). The transpose of a matrix is written by permuting its indices ($\mathbf{X}_{ij}{}^T = \mathbf{X}_{ji}$). To specify a single row and/or column of a matrix, the corresponding index or indices are underlined. For example, the jth column of $\mathbf{X}_{ij}$ is written $\mathbf{X}_{i\underline{j}}$.

3. MODAL EFFECTIVE PARAMETERS

3.1 Frequency Response Functions

The concept of modal effective parameters was developed over several years to overcome difficulties arising in the context of mode superposition by identifying the significant parameters which govern the dynamic phenomena. The effective mass concept was developed in the seventies [6] and used intensely, in particular in the aerospace industry, but it covers only one aspect of the problem. An extension to other modal effective parameters was then proposed in the mid-eighties [7] providing a unified approach for these parameters. Since that time, extensive use of this concept has been made in various fields of structural dynamics [8].

In the context of modal identification, which is the inverse problem of mode superposition, the modal effective parameters can also be used efficiently because of their simple physical role within FRF. A review of this concept for a linear structure with an assumed rigid junction is presented hereafter.

The nature of a given FRF is directly related to the nature of the corresponding excitation and response points or degrees of freedom (DOF). As illustrated in Figure 1, the DOF of a structure may be divided into two mutually exclusive sets:

- the rigid junction DOF, j, with 6 components
- the internal DOF, i with N components

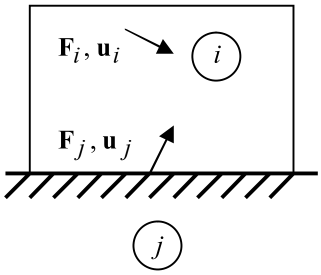

Fig. 1: Structural Degrees of Freedom (DOFs)

The structure may be excited by imposed rigid-body displacements, $\mathbf{u}_j$, at the junction or applied internal forces $\mathbf{F}_i$. The responses include the internal displacements, $\mathbf{u}_i$, and the reaction forces, $\mathbf{F}_j$. In the frequency domain, ω, the relationship between the excitations $\mathbf{F}_i$, $\mathbf{u}_j$ and responses $\mathbf{u}_i$, $\mathbf{F}_j$ can be written in terms of the following FRF

$$\begin{bmatrix} \mathbf{u}_i(\omega) \\ \mathbf{F}_j(\omega) \end{bmatrix} = \begin{bmatrix} \mathbf{G}_{ii}(\omega) & \mathbf{T}_{ij}(\omega) \\ -\mathbf{T}_{ji}(\omega) & -\omega^2 \mathbf{M}_{jj}(\omega) \end{bmatrix} \begin{bmatrix} \mathbf{F}_i(\omega) \\ \mathbf{u}_j(\omega) \end{bmatrix} \quad (1)$$

where **G**, **T**, and **M** are the dynamic flexibility, transmissibility and mass matrices respectively.

3.2 Mode Superposition

Assuming a mode superposition approach, the above FRF may be expressed as a sum over the k modes:

$$\mathbf{G}_{ii}(\omega) \approx \sum_{\underline{k}=1}^{N} H_{\underline{k}}(\omega)\, \widetilde{\mathbf{G}}_{ii,\underline{k}} + \mathbf{G}_{ii,res} \quad (2)$$

$$\mathbf{T}_{ij}(\omega) \approx \sum_{\underline{k}=1}^{N} T_{\underline{k}}(\omega)\, \widetilde{\mathbf{T}}_{ij,\underline{k}} + \mathbf{T}_{ij,res} \quad (3)$$

$$\mathbf{M}_{jj}(\omega) \approx \sum_{\underline{k}=1}^{N} T_{\underline{k}}(\omega)\, \widetilde{\mathbf{M}}_{jj,\underline{k}} + \mathbf{M}_{jj,res} \quad (4)$$

where $H_{\underline{k}}(\omega)$ and $T_{\underline{k}}(\omega)$ are the dimensionless amplification factors of mode $\underline{k}$ and function of the natural frequency, $\omega_{\underline{k}}$, and modal damping ration, $\zeta_{\underline{k}}$

$$H_{\underline{k}}(\omega) = \frac{1}{1 - \left(\dfrac{\omega}{\omega_{\underline{k}}}\right)^2 + i\,2\zeta_{\underline{k}}\dfrac{\omega}{\omega_{\underline{k}}}} \tag{5}$$

$$T_{\underline{k}}(\omega) = \frac{1 + i\,2\zeta_{\underline{k}}\dfrac{\omega}{\omega_{\underline{k}}}}{1 - \left(\dfrac{\omega}{\omega_{\underline{k}}}\right)^2 + i\,2\zeta_{\underline{k}}\dfrac{\omega}{\omega_{\underline{k}}}} \tag{6}$$

and $\widetilde{\mathbf{G}}_{ii,\underline{k}}$, $\widetilde{\mathbf{T}}_{ij,\underline{k}}$, $\widetilde{\mathbf{M}}_{jj,\underline{k}}$ the effective flexibility, effective transmissibility and effective mass matrices for mode $\underline{k}$ and composed of normal modes, $\mathbf{\Phi}_{ik}$, modal participation factors, $\mathbf{L}_{kj}$, and generalized masses, $m_{\underline{k}}$.

$$\widetilde{\mathbf{G}}_{ii,\underline{k}} = \frac{\mathbf{\Phi}_{i\underline{k}}\,\mathbf{\Phi}_{\underline{k}i}}{\omega_{\underline{k}}^2\, m_{\underline{k}}} \quad \text{effective flexibility} \tag{7}$$

$$\widetilde{\mathbf{T}}_{ij,\underline{k}} = \frac{\mathbf{\Phi}_{i\underline{k}}\,\mathbf{L}_{\underline{k}j}}{m_{\underline{k}}} \quad \text{effective transmissibility} \tag{8}$$

$$\widetilde{\mathbf{M}}_{ij,\underline{k}} = \frac{\mathbf{L}_{j\underline{k}}\,\mathbf{L}_{\underline{k}j}}{m_{\underline{k}}} \quad \text{effective mass} \tag{9}$$

The contribution of the higher (truncated) modes is represented by the residual flexibility, transmissibility and mass matrices $\mathbf{G}_{ii,res}$, $\mathbf{T}_{ij,res}$ and $\mathbf{M}_{jj,res}$ deduced from the following summation rules with respect to the static flexibility, $\mathbf{G}_{ii}$, rigid-body junction modes, $\mathbf{\Psi}_{ij}$, and the rigid-body mass matrix, $\overline{\mathbf{M}}_{jj}$.

$$\sum_{\underline{k}=1}^{N} \widetilde{\mathbf{G}}_{ii,\underline{k}} + \mathbf{G}_{ii,res} = \mathbf{G}_{ii} \tag{10}$$

$$\sum_{\underline{k}=1}^{N} \widetilde{\mathbf{T}}_{ij,\underline{k}} + \mathbf{T}_{ij,res} = \mathbf{\Psi}_{ij} \tag{11}$$

$$\sum_{\underline{k}=1}^{N} \widetilde{\mathbf{M}}_{jj,\underline{k}} + \mathbf{M}_{jj,res} = \overline{\mathbf{M}}_{jj} \tag{12}$$

According to equations (2-4), the contribution of each mode to any given FRF may be expressed as the product of a dimensionless amplification factor function of the natural frequency and damping ratio, with the associated modal effective parameter. The effective parameter is real-valued, independent of the normalization of the eigenvectors, has the same dimension and physical units of the corresponding FRF and is directly related to the static response via the summation rules in equations (10-12).

4. MODAL IDENTIFICATION

4.1 Introduction

The purpose of modal identification is to determine via curve-fitting of the measured FRF the three modal quantities - natural frequency, modal damping and modal effective parameters.

In order to better understand the numerous methods which have been developed over the past decades, it is useful to classify them according to 1) the domain (time or frequency) in which the identification is performed, 2) the number of modes which can be simultaneously identified and 3) the number of FRF which can be taken into account. These three classification types are described hereafter.

Frequency domain methods perform curve-fitting on the FRF whereas time domain methods use the IRF (Impulse Response Functions) defined as the response of the structure subjected to a unit impulse excitation, and obtained by the Inverse Fourier Transform of the FRF. Several time domain methods including CE (Complex Exponential), ITD (Ibrahim Time Domain) and ERA (Eigensystem Realization Algorithm) were evaluated at the beginning of this study but did not reveal any advantages over the frequency domain methods. Indeed, the frequency domain methods are particularly well adapted to the given context since 1) the measured FRF may be used directly (no need for FFT) and 2) the FRF offer a much better visual interpretation and physical understanding. For these reasons the study was oriented towards the use of frequency domain methods.

Methods can also be classified according to the number of modes which can be identified. We can therefore distinguish SDOF methods which identify one mode at a time, from MDOF methods capable of identifying several modes simultaneously over a given frequency band. The original RTMVI method is essentially an SDOF method in that the natural frequencies and damping ratios are obtained by "peak-picking" at each selected resonance without taking into account the coupling between modes. If the resonances are well separated, the SDOF approach is adequate. However in some situations the modes may be highly coupled - even in the lower frequencies - as in the case of the first bending modes of a spacecraft structure. The need for MDOF modal identification can be satisfied either by considering an existing MDOF method to be used in addition to RTMVI, or by extending the RTMVI approach to include MDOF capabilities. This was one of the major objectives of the study. Following an initial evaluation of existing frequency domain MDOF methods, the RFP (Rational Fraction Polynomial) method [9] was singled-out for further evaluation for two reasons. First, the RFP method is an industrial standard used in many software codes, and secondly, its algorithm is fully automatic and non-iterative unlike the RTMVI method which is entirely user-driven.

Finally, methods can be classified by the number of the FRF that can be considered. Depending on the number of excitation points (inputs) and response points (outputs) we can speak of SISO (single-input, single-output), SIMO (single-input, multiple-output) and MIMO (multiple-input, multiple-output) FRF measurements. In the context of shaker table vibration tests for a given run along a given direction we are dealing with a single input (imposed base acceleration) and multiple outputs (internal accelerations and possibly interface forces) - thus SIMO FRF. Since the RTMVI method was originally developed for this particular context it is naturally a SIMO method. The RFP method although originally developed as a SISO method has been generalized to a SIMO (and MIMO) version often referred to as the Global Rational Fraction Polynomial (GRFP) method [10].

Although shaker table and modal survey tests both provide FRF, the quality of the FRF obtained from shaker table tests can be substantially degraded for several reasons such as high excitation levels and the presence of notching, high sine-sweep rates affecting the steady-state response, undesirable (parasitic) motion and deformation at the interface, and last but certainly not least the presence of noise.

The next step of the study consisted of comparing the RFP method with the new RTMVI/MDOF method specifically developed for the study. The purpose of the comparison was to determine which method is better suited for MDOF SIMO identification, and in the particular when using FRF obtained from shaker table vibration tests.

These two methods are described hereafter.

4.2 The RFP Method

Consider a set of FRF, $X(\omega)$, where X designates either dynamic transmissibilities, $T(\omega)$, or dynamic masses, $M(\omega)$ for a given base excitation. Equations (3), (4) and (6) can be combined as follows (ignoring the residual term) where $\widetilde{X}_k$ is the modal effective parameter associated with $X(\omega)$.

$$X(\omega) = \sum_{k=1}^{N} \frac{\omega_k^2 + i\,2\zeta_k\,\omega_k\,\omega}{\omega_k^2 - \omega^2 + i\,2\zeta_k\,\omega_k\,\omega}\,\widetilde{X}_k \qquad (13)$$

The FRF of equation (13) may also be expressed using the partial fraction (pole-residue) form in $2N$ space as defined below

$$X(\omega) = \sum_{k=1}^{2N} \frac{A_k}{i\,\omega - \hat{\omega}_k} \qquad (14)$$

where the residues A_k are related to $\widetilde{X}_k$, and the poles, $\hat{\omega}_k$, related to the natural frequency and damping ratio by the following relation.

$$\hat{\omega}_k = \pm\omega_k\sqrt{1-\zeta_k^2} + i\,\zeta_k\omega_k \qquad (15)$$

The system of equations (14) is unfortunately nonlinear in terms of $\hat{\omega}_k$ and therefore cannot be solve directly. To circumvent this problem, the RFP method replaces equation (14) by an equivalent rational fraction involving polynomials $a(\omega)$ and $b(\omega)$.

$$X(\omega) = \frac{a(\omega)}{b(\omega)} = \frac{\sum_{k=0}^{2N-1} a_k\,(i\,\omega)^k}{\sum_{k=0}^{2N} b_k\,(i\,\omega)^k} \qquad (16)$$

Multiplying equation (16) by $b(\omega)$ leads to a linear system in terms of the unknown coefficients a_k and b_k which may be solved using a standard linear least squares approach. In practice, a transformation using orthogonal polynomials to avoid numerical ill-conditioning is applied to equation (17) before solving.

$$e(\omega) = \sum_{k=0}^{2N-1} a_k\,(i\,\omega)^k - \left(\sum_{k=0}^{2N} b_k\,(i\,\omega)^k\right) X(\omega) \qquad (17)$$

Once the optimal coefficients a_k and b_k are computed, then the corresponding poles and residues of equation (14) can be determined using partial fraction expansion - leading finally to the modal terms of equation (13).

As previously stated, the main advantage of the RFP method is that it's fully automatic and non-iterative (no starting solution). In fact, the only required input is the number of modes, *N*, to be identified. However this is perhaps the most critical parameter since the curve-fitting process does not distinguish between genuine modes and artificial or numerical modes which may be present (and necessary) in order to account for noise and discretization errors. Hence the necessity to examine the influence of *N* on the identified modes via stabilization diagrams for example.

The principal drawback of the RFP method lies in its overall sensitivity to noise. This can be illustrated by considering a simple FRF with two distinct resonances. If no noise is present in the data, then the RFP method identifies the two modes without error as shown below in Figure 2 where the initial FRF and synthesized FRF (obtained from the polynomials $a(\omega)$ and $b(\omega)$) are perfectly superposed.

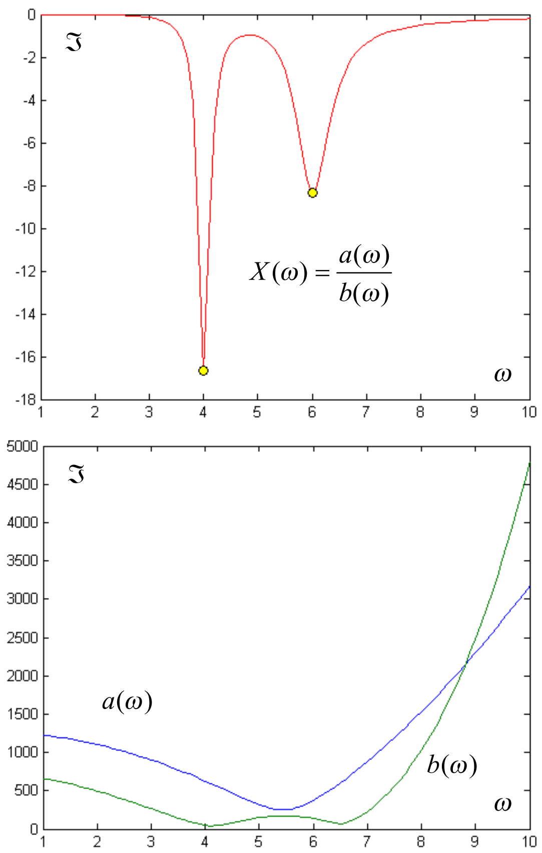

Fig. 2: RFP Identification without Noise

However, if noise is now introduced into the data as illustrated in Figure 3, the identified polynomials $a(\omega)$ and $b(\omega)$ produce a very poor curve-fit especially at the resonances.

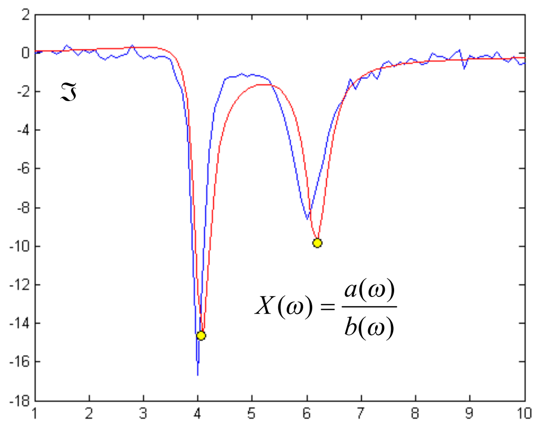

Fig. 3: RFP Identification with noise

This poor fit stems from the linearized system of equation (17) where we see that the FRF $X(\omega)$ are multiplied or *weighted* by the polynomial $b(\omega)$. Moreover, the minima of $b(\omega)$ coincide with the resonances of $X(\omega)$ as illustrated in Figure 2. Therefore the curve-fit obtained from equation (17) will lead to higher discrepancies at points near the resonances - which is exactly the opposite of the desired effect. Corrections to this problem using iterative weighted least-squares solutions have been proposed [11], but their effectiveness depends on the amount of noise and their use defeats the non-iterative nature of the RFP method.

4.3 The RTMVI/MDOF Method

The RTMVI/MDOF method developed in this study is, unlike the RFP method, an iterative procedure driven by the user.

As in original RTMVI method, only the imaginary part of the FRF is used, yielding the following expression derived from equation (13).

$$\Im X(\omega) = \sum_k \frac{-\omega^2 / 2\zeta_k \omega_k^2}{(1-\omega^2/\omega_k^2)^2 + (2\zeta_k)^2} \tilde{X}_k \qquad (18)$$

Rewriting equation (18) for n FRF defined over i frequency points, we obtain equation (19) where $a_k = 1/\omega_k^2$, $b_k = 1/(2\zeta_k)^2$ and $\mathbf{C}_{kn} = \tilde{\mathbf{X}}_{n,k} / \omega_k^2$.

$$\Im \mathbf{X}_{in} = \sum_k \frac{a_k \omega_i^2}{b_k (1 - a_k \omega_i^2)^2 + 1} \mathbf{C}_{kn} \qquad (19)$$

Finally, equation (19) can be expressed in matrix form by introducing the matrix $\mathbf{D}_{ik}$.

$$\Im \mathbf{X}_{in} = \mathbf{D}_{ik} \mathbf{C}_{kn} \qquad (20)$$

with $\mathbf{D}_{ik} = \dfrac{a_k \omega_i^2}{b_k (1 - a_k \omega_i^2)^2 + 1}$ (expanded over i and k)

With the RTMVI/MDOF method, the user starts by performing a "manual" identification of one or several modes over a selected frequency interval. The manual identification consists of graphically determining a set of modes (ω_k, ζ_k, and $\tilde{\mathbf{X}}_{n,k}$) in order to obtain a satisfactory set of synthesized responses compared to the measured responses. The user decides the number of modes he or she wishes to create and the corresponding natural frequency and damping (ω_k, ζ_k).

The modal effective parameters, $\tilde{\mathbf{X}}_{n,k}$, are determined automatically (and interactively) by solving equation (20) for $\mathbf{C}_{kn}$ via a least-squares solution. As the user adjusts the modal parameters (ω_k, ζ_k), the modal effective parameters are updated and the corresponding synthesized responses are computed and plotted - all interactively.

This manual identification is illustrated in Figure 4 for a single FRF with two modes. The measured and synthesized FRF are plotted in blue and red respectively. The modes are depicted by the vertical green lines which can be modified interactively by the user. Horizontal displacement of the mode lines modifies the natural frequency whereas moving the curser vertically over a given line increases or decreases the modal damping ratio.

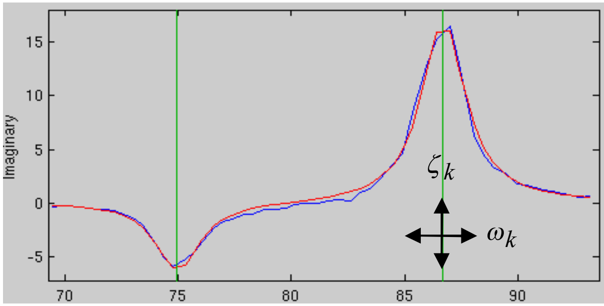

Fig. 4: RTMVI Manual Identification

In some cases, it may be desirable to have all three modal parameters (ω_k, ζ_k, and $\tilde{\mathbf{X}}_{n,k}$) automatically computed with respect to an initial set of values. In this case equation (20) is solved via nonlinear least-squares using a conjugate gradient method (e.g. Davidon-Fletcher-Powell) with physical bounds imposed on b_k such that the corresponding damping values ζ_k remain positive. The advantage of a gradient-based approach in this context is that the derivatives of $\mathbf{D}_{ik}$ and $\mathbf{C}_{kn}$ are available analytically and easy to derive. Therefore gradients can be quickly determined resulting in a reasonably fast optimization procedure - even when using a large number of modes and responses.

An important new feature of the RTMVI/MDOF method is the use of SVD (singular value decomposition) to facilitate and improve FRF assessment and subsequent modal identification - particularly when dealing with a large number of FRF.

The imaginary part of the FRF $\mathbf{X}(\omega)$ may be decomposed into a product of orthonormal responses, $\mathbf{U}(\omega)$, a diagonal matrix of principal values, **S**, and an orthonormal matrix, **V**.

$$\Im\mathbf{X}(\omega) = \mathbf{U}(\omega)\,\mathbf{S}\,\mathbf{V}^T \tag{21}$$

If we define the PRF (Principal Response Functions), $\mathbf{P}(\omega)$, as the product $\mathbf{U}(\omega)\,\mathbf{S}$, we see that the physical and principal responses are simply linear combinations of each other via the orthonormal matrix, **V.**

$$\mathbf{P}(\omega) = \Im\mathbf{X}(\omega)\,\mathbf{V} \tag{22}$$

$$\Im\mathbf{X}(\omega) = \mathbf{P}(\omega)\,\mathbf{V}^T \tag{23}$$

The principal values in **S**, indicate the rank (degree of independence) of the responses. Often, the rank of the responses is much less than the number of responses. This allows representing a large number of physical responses by a just a small number of principal responses.

Moreover, since the PRF are linear combinations of the FRF, they conserve the modal properties (natural frequency and damping) of the physical system. Therefore, modal identification can be performed using the PRF - resulting in the following advantages:

- Improved interpretation and comprehension by working with a small number of independent (and orthogonal) principal responses
- Improved numerical performance during modal identification for the same reasons.
- The number of non-zero principal values or response can be used as an estimate of the *minimum* number of modes present in the selected frequency range.

The FRF and PRF are illustrated in Figure 5 for a frequency band including two modes. Modal identification can be performed more easily and faster by using only the two non-zero PRF.

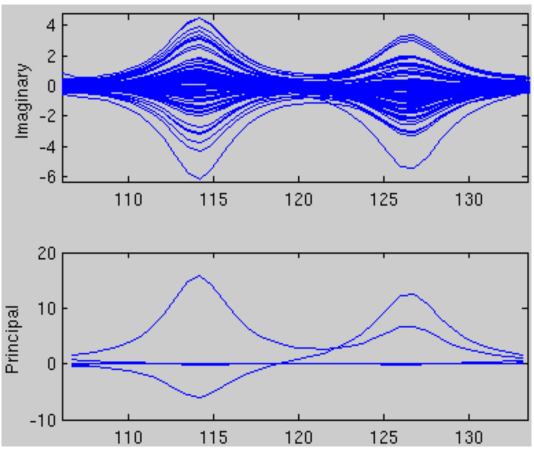

Fig. 5: FRF and PRF

4.4 Choice of Method

In the context of shaker table tests where the quality of FRF is often degraded compared to measurements from modal survey tests, it is advantageous for the user to maintain control of the identification process in order to achieve the best results. Consequently, the user-driven graphical approach of the RTMVI/MDOF method has proven more robust and accurate than the automatic and less intuitive RFP method. Moreover with the use of SVD, the RTMVI/MDOF method remains highly efficient in spite of its nonlinear nature. The RTMVI/MDOF method was therefore chosen to be integrated in the PRIMODAL software code [12] and validated using the PICARD micro-satellite structure. A summary of the validation is presented hereafter.

5. INDUSTRIAL APPLICATION

The PICARD FE model and experimental mesh showing the location of the 88 accelerometers is presented in Figure 6.

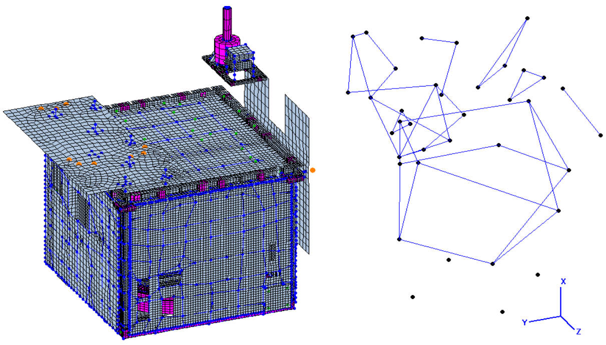

Fig. 6: PICARD FE Model and Instrumentation

An initial validation study of the RTMVI/MDOF method was carried out using *simulated* FRF from the FE model with a lateral (Z-direction) base excitation. A total of 14 modes were identified in five different frequency bands illustrated in Figure 7.

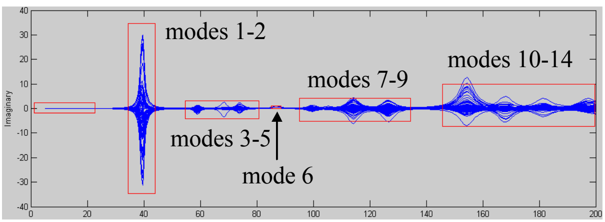

Fig. 7: Simulated FRF and Frequency Bands

To illustrate the method's capability of identifying coupled modes, consider the frequency band at approximately 40 Hz where both fundamental bending modes of the structure are excited and highly coupled as illustrated in Figure 8. The FRF are plotted in the top graphs - alone at left and with the synthesized FRF superposed in red at right. The corresponding PRF are plotted in the bottom graphs with the PRF synthesis at right. The two identified modes indicated by the green mode lines are separated by less than 0.5 Hz.

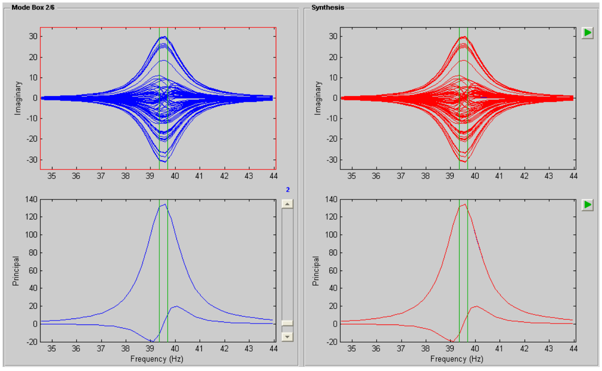

Fig. 8: Identification of Coupled Modes

By working with the PRF, it was possible to identify the two coupled modes manually - without the need to perform nonlinear optimization - thus demonstrating the capabilities of the method.

The comparison between the identified modes and the reference modes of the FE model are tabulated in Figure 9 in terms of frequency errors damping values and MAC. The modal parameters show excellent agreement over all identified modes.

Model: picard_fem
Ref. : picard_sim_z

No.	Model (Hz)	(zz)	No.	Reference (Hz)	(zz)	Freq. (% Err)	MAC
1	39.345	0.0400	1	39.345	0.0400	0.00	1.00
2	39.689	0.0400	2	39.689	0.0400	-0.00	1.00
3	58.917	0.0400	3	58.915	0.0405	0.00	1.00
4	68.286	0.0400	4	68.285	0.0404	0.00	1.00
5	73.804	0.0400	5	73.805	0.0401	-0.00	1.00
6	86.884	0.0400	6	86.884	0.0415	0.00	1.00
7	99.566	0.0400	7	99.564	0.0402	0.00	1.00
9	105.412	0.0400	8	105.350	0.0400	0.06	0.99
11	114.090	0.0400	9	114.085	0.0401	0.00	1.00
12	126.465	0.0400	10	126.468	0.0402	-0.00	1.00
14	154.306	0.0400	11	154.305	0.0400	0.00	1.00
15	167.895	0.0400	12	167.887	0.0400	0.00	0.99
18	181.365	0.0400	13	181.263	0.0425	0.06	1.00
20	197.380	0.0400	14	197.483	0.0451	-0.05	0.99

Fig. 9: Comparison Simulated Test / Analysis

A second validation study was performed using the measured FRF obtained from a low-level lateral (Z) run. A total of 9 modes were identified in 4 frequency bands illustrated in Figure 10.

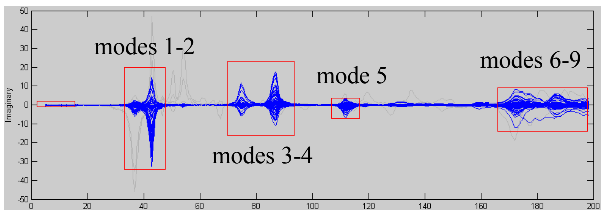

Fig. 10: Measured FRF and Frequency Bands

The identification of the last 4 modes is illustrated in Figure 11. In spite of the noise that is clearly visible in the FRF, modes can be identified with a relatively good curve-fit in both the FRF and PRF.

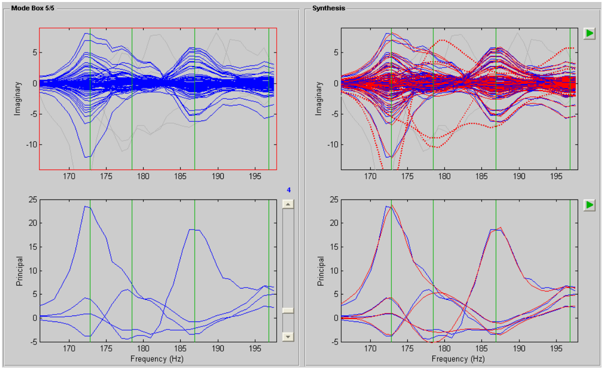

Fig. 11: Identification of Coupled Modes with Noise

For completeness, the comparison of the identified modes and the FE model is presented in Figure 12 and indicates the need for subsequent model updating.

Model: picard_fem
Ref. : picard_bn_y

No.	Model (Hz)	(2z)	No.	Reference (Hz)	(2z)	Freq. (% Err)	MAC
2	39.689	0.0400	1	36.900	0.0750	7.56	0.74
1	39.345	0.0400	2	42.803	0.0376	-8.08	0.52
3	58.917	0.0400	3	74.867	0.0338	-21.30	0.97
5	73.804	0.0400	4	86.778	0.0257	-14.95	0.95
7	99.566	0.0400	5	111.970	0.0259	-11.08	0.93
13	134.568	0.0400	6	172.822	0.0297	-22.13	0.52
17	172.274	0.0400	7	178.448	0.0567	-3.46	0.38
18	181.365	0.0400	8	186.885	0.0328	-2.95	0.26
14	154.306	0.0400	9	196.835	0.0342	-21.61	0.49

Fig. 12: Comparison Test / Analysis

6. CONCLUSIONS

A study has recently been carried out for the CNES/Toulouse with the goal of enhancing the RTMVI modal identification method following ten years of industrial use in the aerospace field.

The improvements include an extension to an MDOF formulation in order to identify coupled modes and the use of SVD to improve FRF assessment as well as the modal identification process especially when working with a large number of FRF. The resulting RTMVI/MDOF method has been implemented in the PRIMODAL structural analysis code and validated using the PICARD micro-satellite structure.

7. REFERENCES

[1] Cahier des clauses Techniques Particulières de l'étude libre : *Identification modal sur essais sinus à but de recalage de modèles*, Document CNES, Réf DCT/TV/SM-2008-NT-4704 Ed. 2, 04 Septembre 2008.

[2] Ewins, D.J., *Modal Testing - Theory, Practice and Application*, Research Studies Press, Edition 2, 2001.

[3] Maia, N.M., Sylva J.M. et al, *Theoretical and Experimental Modal Analysis*, Research Studies Press, 1997.

[4] Girard A., Roy N., Guyot M., Bugeat L.-P., *Modal Identification via Effective Parameters: An Industrial Solution*, European Conference on Spacecraft Structures, Materials and Mechanical Testing, Proceedings ESA SP-468, p. 283-288, March 2001.

[5] Lefevre Y.M., Bonetti J.C., Girard A., Roy N., Calvi A., , *Real Time Modal Identification Techniques for Improved Satellite Vibration Testing*, Proceedings, European Conference on Spacecraft Structures, Materials and Mechanical Testing, Toulouse, France, Dec. 2002.

[6] R.M. Bamford, B.K. Wada, and J.A. Garba, "Equivalent spring-mass system for normal modes," Technical memorandum 33-380, Jet Propulsion Laboratory, Feb. 1971.

[7] A. Girard, J.F. Imbert "Modal Effective Parameters and Truncation Effects in Structural Dynamics," Proceedings of the 5th International Modal Analysis Conference, London, April 1987.

[8] GIRARD A., ROY N., *Structural Dynamics in Industry*, ISTE Ltd and John Wiley & Sons, ISBN 978-1-84821-004-2, 2008.

[9] Richardson, M.H., Formenti, D.L., *Parameter Estimation from Frequency Response Measurements using Ration al Fraction Polynomials*, Proc. 1st Int. Modal Analysis Conference, Orlando, FL, pp. 167-181, 1982.

[10] Richardson, M.H., Formenti, D.L., *Global Curve-fitting of Frequency Response Measurements using the Rational Fraction Polynomial Method*, Proc. 3rd Int. Modal Analysis Conference, Orlando, FL, pp. 390-397, 1985.

[11] Deschrijver, D. and Dhaene, T., *Iterative Rational Least-Squares Method for Efficient Transfer Function Synthesis*, Proceedings of the 17th International Symposium on Mathematical Theory of Networks and Systems, Kyoto, Japan, July 24-28, 2006.

[12] *PRIMODAL User's Manual*, Version 1.8, Ref. Top Modal D0409271, July 21 2009.